

RESEARCH PAPER

Synthesis, characterization and sonophotocatalytic degradation of an azo dye on Europium doped cadmium selenide nanoparticles

Younes Hanifehpour* and Sang Woo Joo*

School of Mechanical Engineering, Yeungnam University, Gyeongsan 712-749, Korea

ARTICLE INFO

Article History:

Received 6 April 2018

Accepted 14 July 2018

Published 1 August 2018

Keywords:

Europium

Nanomaterials

Sonophotocatalytic

Degradation

ABSTRACT

In this study, Eu-doped CdSe nanoparticles with variable Eu^{3+} content were synthesized by a simple sonochemical method. Eu^{3+} substitution into the structure of CdSe resulted in a material with new physical properties, composition and morphology. The synthesized nanoparticles were characterized by powder X-ray diffraction (XRD), scanning electron microscopy (SEM), X-ray photoelectron spectroscopy (XPS), Brunauer–Emmett–Teller (BET), and UV-Vis diffuse reflectance spectroscopy techniques. The sonocatalytic efficiency of pure and $\text{Eu}_x\text{Cd}_{1-x}\text{Se}$ samples was evaluated by monitoring the decolorization of RRed 43 in aqueous solution under visible light irradiation. The BET specific surface area and pore volume of mesoporous europium doped CdSe greatly exceeds in comparison to undoped CdSe samples. Among the different amounts of dopant, 8% Eu-doped CdSe showed the highest catalytic activity. The effects of various parameters such as initial dye concentration, catalyst loading, ultrasonic power, and the presence of radical scavengers were investigated. Superoxide radicals and photogenerated holes were detected as the main oxidative species.

How to cite this article

Hanifehpour Y. Synthesis, characterization and sonophotocatalytic degradation of an azo dye on Europium doped cadmium selenide nanoparticles. *Nanochem Res*, 2018; 3(2):178-188. DOI: 10.22036/ncr.2018.02.007

INTRODUCTION

Degradation of hazardous organic pollutants existing in industrial wastewater via advanced oxidation processes (AOPs) has been an active area of research. The primary mechanism of AOP is production of $\bullet\text{OH}$ radical with high oxidization potential to achieve faster and efficient degradation of the contaminants. The AOP procedure is particularly appropriate for cleaning biologically toxic or non-degradable materials such as aromatics, pesticides, petroleum constituents, and volatile organic compounds in wastewater [1–4]

In the recent years, sonocatalysis as another AOP process has also been applied for degradation of organic dyes [5–7]. The chemical influence of ultrasonic (US) arises from acoustic cavitation include the formation, growth and implosive collapse of bubbles in a solution. The collapse of

bubbles produces localized hot spot with very high temperature and a pressure. Under such extreme conditions, the dissolved oxygen and water molecules can undergo direct thermal dissociation to produce highly reactive radical species such as ($\bullet\text{OH}$), hydrogen ($\bullet\text{H}$) and oxygen ($\bullet\text{O}$), that play an important role in oxidizing organic pollutants in water [8–11].

Unification of these two methods together seems to enhance the degradation ratio of organic pollutants due to the synergic effect of sonocatalysis and photocatalysis [12]. Alongside the formation of reactive oxygen species (ROS) via cavitation, the use of ultrasound wave in photocatalytic process have other benefits such as increasing the active surface area of catalyst by preventing the aggregation of particles, increasing the mass transfer of pollutants between solution and catalysts surface, preventing

* Corresponding Authors Email: younes.hanifehpour@gmail.com
swjoo@yu.ac.kr

the catalyst deactivation by continuously cleaning the catalyst surface from absorbed molecules by microstreaming and micro bubbling, and increasing the number of regions of high temperature and pressure by breaking up microbubbles created via US into smaller ones in the presence of catalyst particles [13–14].

Among the II–VI semiconducting materials, CdSe has been extensively investigated owing to its small band gap energy, which has been reported to be from 1.65 to 1.8 eV [15]. It has been found to be suitable for various optoelectronic applications in catalysis [16], biological labeling [17] and solar cells [18]. CdSe has been regarded as an efficient semiconductor under visible light irradiation [15]. However the fast recombination of photogenerated electron-holes restricted its practical application because the photoinduced electrons and holes are neutralized before they can initiate the photocatalytic processes [19]. Lanthanide-doped nanostructured semiconductors have been utilized as an effective photocatalyst and sonocatalyst in recent years. Rare earth cations with incomplete occupied 4f and empty 5d orbitals also could notably improve the separation rate of photo induced charge carriers in semiconductor sonocatalysts and greatly enhance the sonocatalytic activity [1,20–22].

In this study, a simple sonochemical route is introduced for the synthesis of pure and europium-doped CdSe ($\text{Eu}_x\text{Cd}_{1-x}\text{Se}$) nanoparticles. The sonocatalytic activity of pure and Eu-doped CdSe nanoparticles was investigated toward to RRed 43 (as a model organic dye) (see Table 1). There is no report on the sonocatalytic degradation of RRed 43 in the presence of Eu-doped CdSe nanoparticles.

EXPERIMENTAL SECTIONS

Chemicals and materials

All chemicals needed in this study were of analytical grade and were used without further

purification. Se (99.99 %), $\text{Eu}(\text{NO}_3)_3 \cdot 5\text{H}_2\text{O}$, ethanol (99 %) and NaOH were obtained from Sigma-Aldrich. $\text{Cd}(\text{NO}_3)_2 \cdot 4\text{H}_2\text{O}$ (99.5 %) and $\text{N}_2\text{H}_4 \cdot \text{H}_2\text{O}$ (99 %) were purchased from Merck; Reactive Red 43 was obtained from the Zhejiang Yide Chemical Company (China).

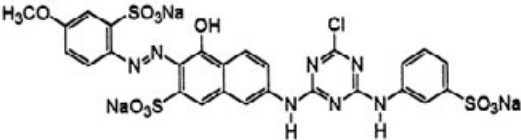
Preparation of Eu-doped CdSe nanoparticles

Eu-doped cadmium selenide compounds with different Eu contents (0–12 mol %) were prepared through sonochemically route using hydrazine hydrate ($\text{N}_2\text{H}_4 \cdot \text{H}_2\text{O}$) as the reducing agent. In a usual synthesis, $\text{Cd}(\text{NO}_3)_2 \cdot 4\text{H}_2\text{O}$ and appropriate molar ratios of $\text{Eu}(\text{NO}_3)_3 \cdot 5\text{H}_2\text{O}$, 2 mmol Se powder and 1 mmol NaOH were first dissolved in 50 ml distilled water. Then, hydrazine hydrate ($\text{N}_2\text{H}_4 \cdot \text{H}_2\text{O}$) was added drop wise to the above solution with middle speed stirring. Lastly, using bath type sonicator (SW12H, Fisher Scientific) with a frequency of 37 kHz and output intensity of 200 W, the mixture was sonicated for 2h. As-prepared $\text{Eu}_x\text{Cd}_{1-x}\text{Se}$ nanoparticles were collected and washed several times with absolute ethanol and distilled water to remove residual impurities, and then vacuum-dried at 50 °C for 3 h. As a result, the black powder with 84% yield was obtained.

Characterization

To conclude the crystal phase composition of the prepared CdSe and Eu-doped CdSe samples, XRD characterization was carried out at room temperature using a D8 Advance, Bruker, Germany diffractometer with monochromatic high-intensity Cu K α radiation ($\lambda=1.5406 \text{ \AA}$), the accelerating voltage of 40 kV and the emission current of 30 mA. The morphologies and nanostructures of the samples were examined by field emission scanning electron microscope (FESEM, Hitachi S-4200, Japan). X-ray photoelectron spectroscopy (XPS) (K-ALPHA, UK) was used for determination of

Table 1. Characteristics of Reactive Red 43

Chemical structure	
Molecular formula	$\text{C}_{26}\text{H}_{17}\text{ClN}_7\text{Na}_3\text{O}_{11}\text{S}_3$
Molecular weight	804.07 (g/mol)
Chemical class	Single azo class
C.I. number	179125

the chemical composition and chemical state. The optical absorption spectra of all the samples were carried out by diffuse reflectance UV-Vis spectrophotometer (Varian Cary 3 Bio, Australia).

Evaluation of catalytic activity

The sonophotocatalytic activity of undoped and Eu-doped CdSe nanoparticles was evaluated by the decolorization of Reactive Red 43 as a dye pollutant. In a usual process, 0.1g of the nanocatalyst was suspended into 100 mL of model dye aqueous solution with a known initial concentration. Then, the suspended solution was irradiated by compact 40W fluorescent visible lamp equipped with cutoff filter for providing visible light illumination ($\lambda > 420$ nm) in the ultrasonic bath. The evaluation of color removal was determined by its absorbance at $\lambda_{\max} = 519$ nm using UV-Vis spectrophotometer. The decolorization efficiency (DE) was calculated using Eq. 1:

$$DE (\%) = \left(1 - \frac{C}{C_0}\right) \times 100 \quad (1)$$

where C_0 and C are the initial and final concentration of the dye in the solution (mg/L), respectively. In the reusability test of the nanocatalyst, the used catalyst was separated from solution and washed with distilled water and dried at 70 °C and then used in a new experiment.

RESULTS AND DISCUSSION

Characterization of the synthesized samples

The powder X-ray diffraction (P-XRD) patterns

of the Eu-doped CdSe samples are shown at Fig. 1. All the diffraction peaks of the samples can be readily indexed to the pure typical well-crystallized hexagonal CdSe ((No. 08-0549, space group P63mc, $a = 0.4299$ nm and $c = 0.7010$ nm) [20,21] (see supplementary data S1). No peaks showing impurities were identified, confirming that the sonochemical route applied in this study was affluent in synthesizing the desired samples. Moreover, the sharp diffraction peaks in the XRD spectra of the synthesized samples show that the as-prepared compound was highly crystalline. Behind the doping levels of $x = 0.08$ for Eu^{3+} , additional unknown phases were observed. There is a slight shift to the higher diffraction angles in the 0.08% Eu-doped CdSe pattern.

To clarify the size and shape of the nanoparticles, SEM analyses were done. Fig. 2 shows the SEM microphotographs of the CdSe and Eu doped CdSe samples, respectively. As compared to pure CdSe, SEM images display the bigger crystalline size of the europium doped CdSe nanoparticles. This proves that doping of Eu^{3+} ions into the CdSe lattice raises the aggregation of nanoparticles and correspondingly increases the size of the particles.

Figs. 3(a) and (b) show that the size distribution of the $\text{Eu}_{1-x}\text{Cd}_x\text{Se}$ as-synthesized compound is in the range of 40 to 60 nm, which is bigger than that of undoped CdSe nanoparticles (20-40 nm). These figures validate the fact that doping of Eu^{3+} into the structure of CdSe does not change the morphology of CdSe nanoparticles.

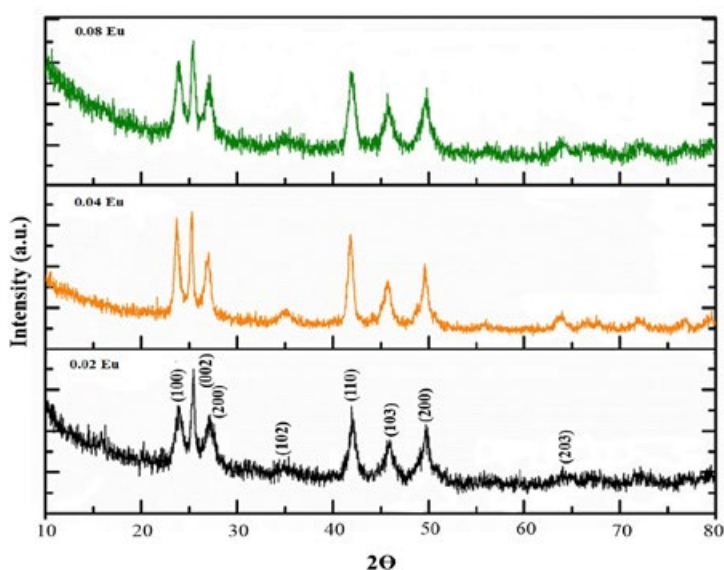


Fig. 1. Powder X-ray diffraction pattern of $\text{Eu}_x\text{Cd}_{1-x}\text{Se}$ ((a) $x = 0.20$, (b) $x = 0.04$, (c) $x = 0.08$)

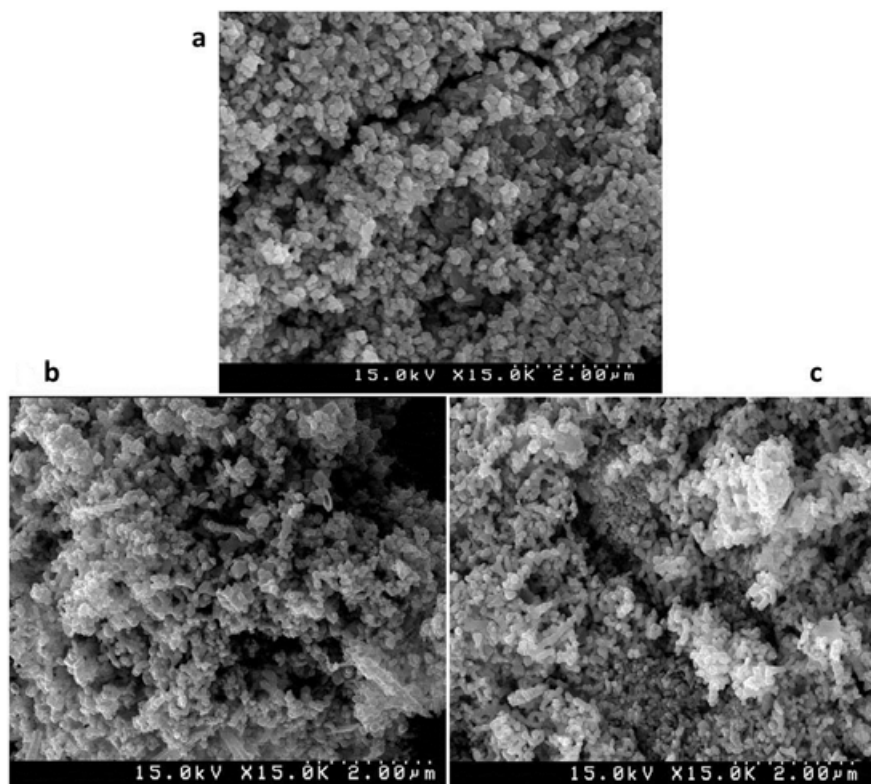


Fig. 2. SEM image of pure CdSe (a), $\text{Eu}_{0.02}\text{Cd}_{0.98}\text{Se}$ (a) and $\text{Eu}_{0.08}\text{Cd}_{0.92}\text{Se}$ (b) nanoparticles

To confirm the incorporation of Eu ions into the CdSe crystal lattice and to evaluate the oxidation state of terbium, XPS analysis was carried out. The XPS spectrum and narrow scan XPS of $\text{Eu}_{0.08}\text{Cd}_{0.92}\text{Se}$ nanoparticles is shown at Fig. 4a–c. As can be seen in narrow scan spectrum of Cd 3d in Fig. 4b, two peaks centered at 405 and 412 eV can be attributed to the transition of Cd $3d_{5/2}$ and Cd $3d_{3/2}$, respectively [23]. The single peak located at the binding energy of 54.58 eV attributed to the Se 3d transition (see Fig. 4b) [24]. As can be seen in Fig. 4c, the presence of Eu $3d_{5/2}$ and $3d_{3/2}$ peaks located at 1134.3 and 1164.2 eV confirms that Eu ions have been successfully doped into the crystal lattice of CdSe [7].

Fig. 5 displays Tauc plot of $(h\nu\alpha)^2$ versus $(h\nu)$ and the intercept of the resulting linear region with the energy axis in which the band gap energy of as-prepared compound can be calculated. It can be concluded that the E_g value of the doped CdSe is lower than that in pure sample, and decreases with the increase of dopant. Table 2 lists the direct optical band gap energy for pure and Eu-doped CdSe.

The nitrogen adsorption/desorption isotherm of the pure CdSe and 8% Eu^{3+} -substituted CdSe

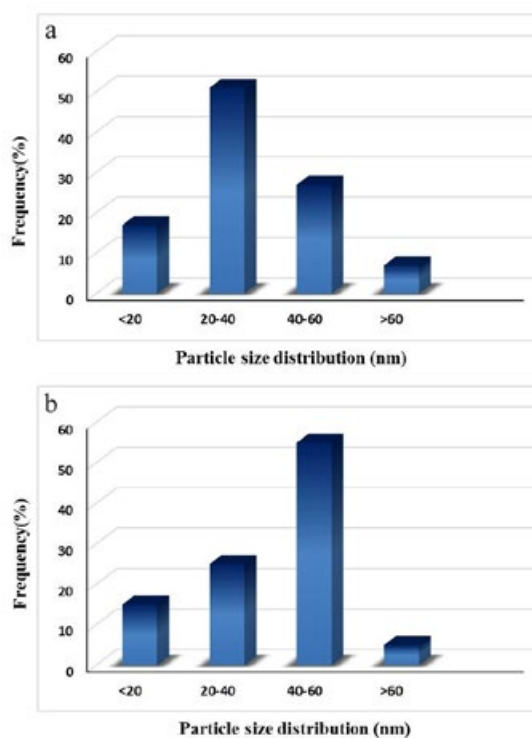


Fig. 3. Particle size distribution profile of (a) undoped CdSe and (b) 8% Eu-doped CdSe nanoparticles.

are shown in Fig. 6. In the case of CdSe and Eu-doped samples, two isotherms with a well-defined hysteresis loop in the pressure range of 0.3–1.0 p/p₀ were observed. The BET specific surface area of mesoporous CdSe is 54.4115m²/g. Also, the BET specific surface area of mesoporous Eu-substituted CdSe (79.3512 m² g⁻¹) considerably exceeds that of CdSe. These physical features expect superior adsorption performances of europium-doped CdSe.

Synergistic effect of photocatalysis and sonocatalysis in degradation of RRed 43 on Eu-doped CdSe

To evaluate the sono, photo and sono-photocatalytic performance of the synthesized Eu-doped CdSe, a set of comparative experiments were conducted and the results are shown in Fig. 7a. As clearly shown, the decolorization efficiency was negligible in the absence of catalyst particles under light irradiation, showing that photolysis

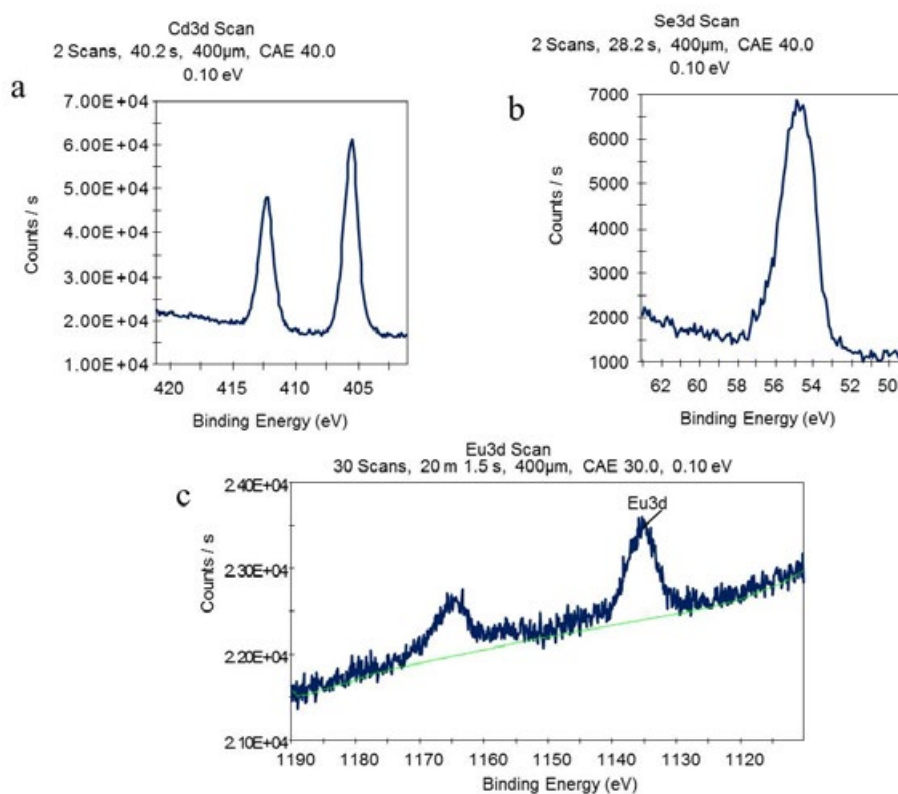


Fig. 4. XPS pattern of 8% Eu-doped CdSe nanoparticles

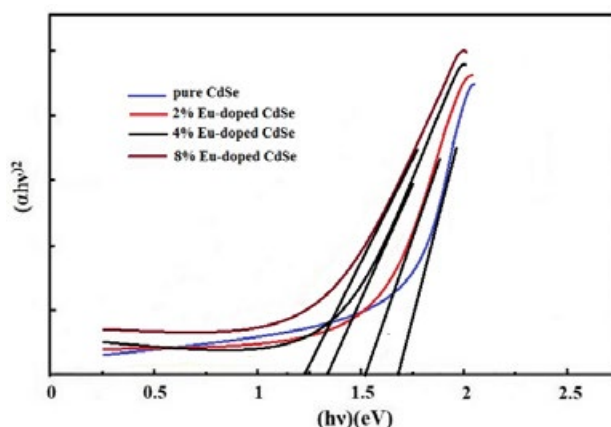


Fig. 5. $(Ahv)^2 - hv$ curves of the undoped and Eu-doped CdSe nanostructures

does not contribute to removal of RRed 43 from aqueous solution. The result of the experiment performed in dark condition indicated that surface adsorption does not have any significant influence in decolorization of dye solution. The removal percentage by photocatalytic process was less than 45% showing the low efficiency of this process. The results of degradation of dye molecules under ultrasonic irradiation in the presence and absence of catalyst particles illustrated that decolorization efficiency by sonocatalytic degradation (69%) was greater than that by the sonolysis process (8%). The decolorization efficiency enhanced significantly in sono-photocatalytic process (89%), because of the synergic effects between sono and photocatalysis which can be summarized as follows: (i) generation more number of ROSs by combined photocatalytic process and cavitation effect, (ii) enhancing the mass transfer rate, (iii) disaggregation of catalyst particles by US wave and more available active surface area, and (iv) formation of more hot spots in the presence of catalyst particles [12–14].

As demonstrated in Fig. 7b, the plot of $(-ln(C/C_0))$ vs. time gives a linear dependence in the case of all three photocatalytic, sonocatalytic and sono-

photocatalytic processes indicating pseudo-first order kinetics.

The changes in the UV-Vis absorption spectra of RRed 43 during the sonophotocatalytic process at different irradiation times are shown in Fig. 8. The decreasing concentration of RRed 43 during the catalytic reaction is used to evaluate the activity of the sonophotocatalyst.

The effect of scavengers on decolorization efficiency

In order to investigate the mechanism of degradation process and to detect the major oxidative species, the experiments were performed

Table 2. Direct optical band gap energy of undoped CdSe and Eu-doped CdSe nanostructures

Sample	Band gap (eV)
Undoped CdSe	1.67
2% Eu-doped CdSe	1.53
4% Eu-doped CdSe	1.36
8% Eu-doped CdSe	1.24

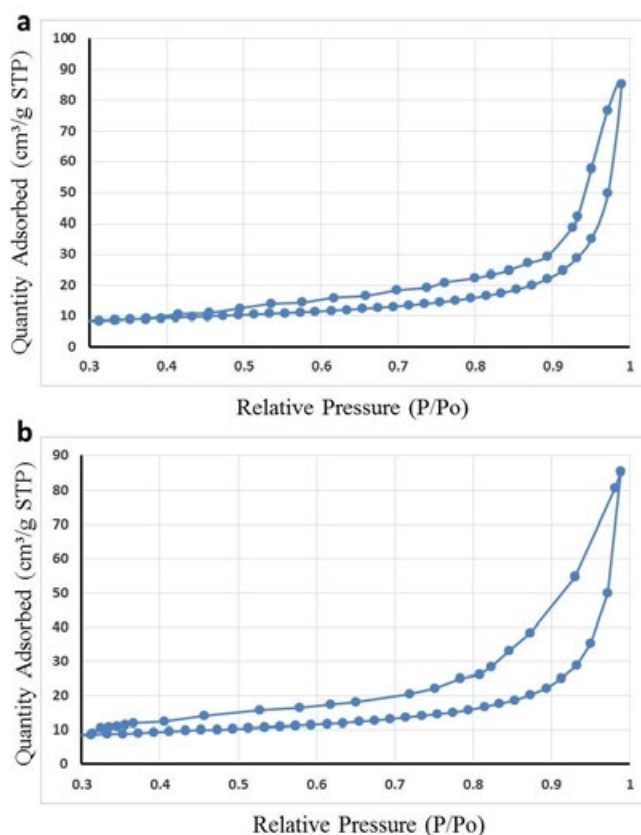
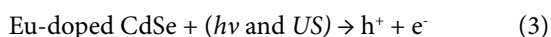


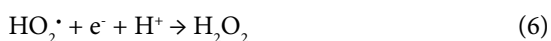
Fig.6. Typical nitrogen adsorption–desorption isotherm of mesoporous pure CdSe (a) and 8% Eu-doped CdSe (b).

in the presence of suitable scavengers of active species. As presented in Fig. 9, addition of t-BuOH (the scavenger for hydroxyl radical) causes 37% decrease in decolorization percentage. With the addition of oxalate (scavenger for h^+_{VB}) the decolorization percentage reduced to 57%. When benzoquinone (BQ) (scavengers for superoxide radicals) was added, degradation of dyes is remarkably inhibited. These results indicated that superoxide radicals and h^+_{VB} were the main oxidative species in degradation of dye molecules, however, hydroxyl radicals affect the decolorization too. Considering the synergic effect of sono and photocatalysis and above discussion, the possible mechanism for degradation process can be as follows [12,14]:

i) The catalyst nanoparticles can get excited by both light and US irradiation to generate electron-hole pairs:



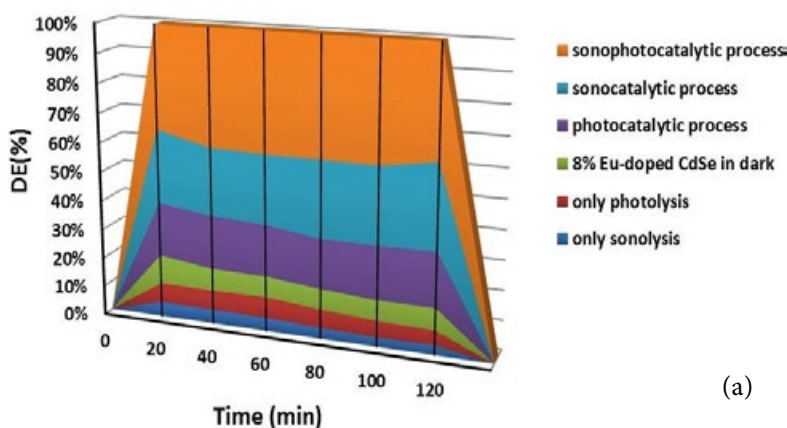
ii) The conduction band electron can react with adsorbed oxygen molecules to form $\cdot O_2^-$, $HO_2\cdot$ and H_2O_2 :



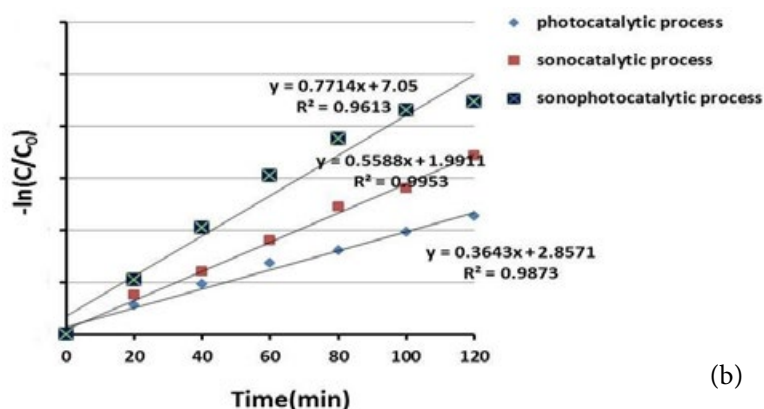
iii) The photogenerated holes can oxidize the water molecules or hydroxyl anions to constitute hydroxyl radicals:



iv) Also the presence of ultrasonic irradiation can promote water molecule pyrolysis and produce hydroxyl and hydrogen radicals:



(a)



(b)

Fig. 7. (a) Comparison of different processes in decolorization of Reactive Red43, (b) First order kinetic plot for photocatalytic, sonocatalytic and sono-photocatalytic processes. [Dye] = 10 mg/L, [Catalyst] = 1.5 g/L

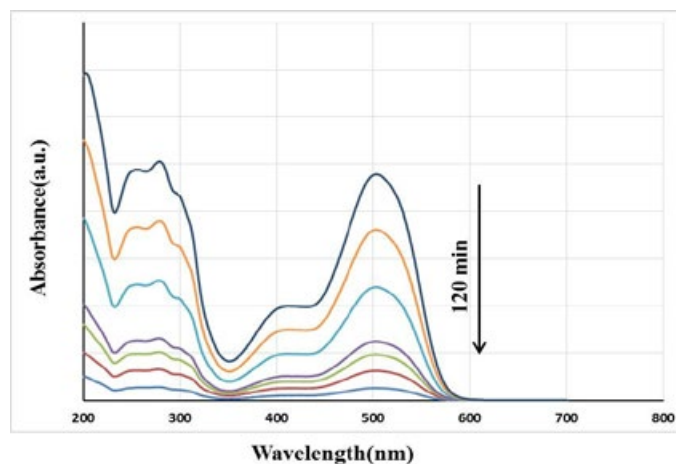


Fig.8. Degradation of RRed 43 under sonophotocatalytic process using 8% Eu-doped CdSe nanoparticles.

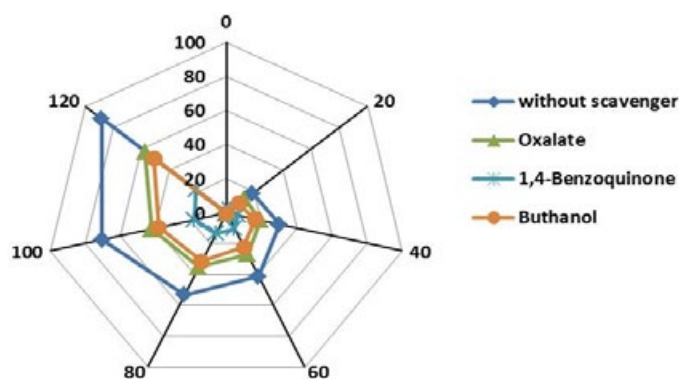
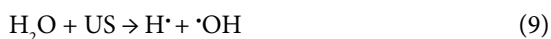
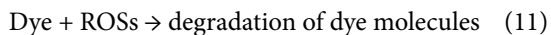


Fig. 9. Effect of different scavengers on decolorization of Reactive Red 43, [Dye] = 10 mg/L, [Catalyst] = 1.5 g/L, [Scavenger] = 5 mM



(v) Finally, the produced active species can degrade the dye molecules:



Influence of primary dye concentration

In this study, different initial dye concentrations, varying from 10 to 40 mg/L, were employed. As displayed in Fig. 10, DE% decreased from 88.32 to 59.14% considering primary concentration from 10 to 40 mg/L. At high dye concentrations, the pollutant molecules fill the energetic sites on the surface of the catalyst and led to a remarkable reduction in the degradation ratio. The diffusion of light to the catalyst's surface may be prevented in the elevated concentration of dye solution causing lower performance. [25].

Influence of catalyst amount

Fig. 11 displays the influence of catalyst dosage on the degradation ratio. Initial dye concentration and sonication time were continual at 10 mg/L and 120 min, respectively. From Fig. 12, the color removal ratio was 57.32, 72.36, 89.35 and 82.10 % at dosages of 0.5, 1, 1.50 and 2 g/L, respectively. Therefore, the degradation ratio elevated from 0.5 to 1.50 g/L, and afterwards reduced. This trend could be assigned to the extending active surface area for the sonication process. Due to the aggregation of sonocatalyst which reduces the number of active sites and ultrasound scattering, DE% decreases beyond 1 g/L [5, 12].

Influence of sonication power

The influence of ultrasonic power on the decolorization ratio of RRed 43 was also studied in the range from 50 to 200 W. The degradation ratio is elevated from 62.33 % to 93.52% with applying

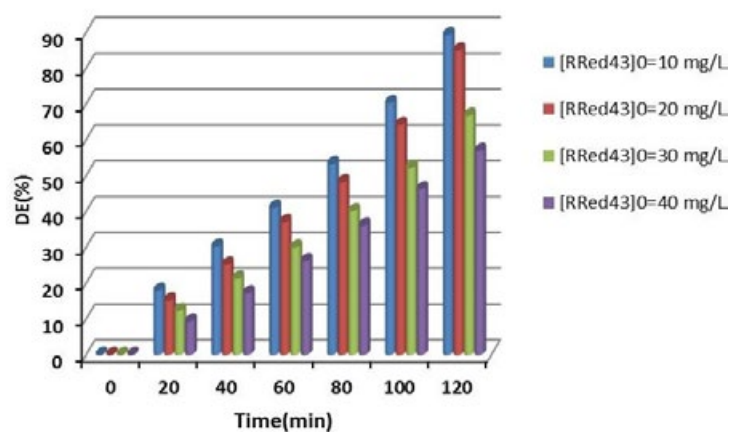


Fig. 10. The influence of RRed 43 concentration on degradation efficiency.

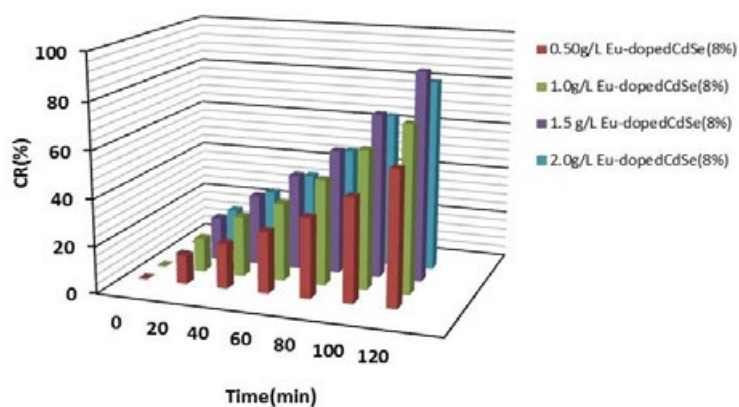


Fig.11. Influence of 8% Eu-doped CdSe concentration on the decolorization of 10 g/L RRed 43.

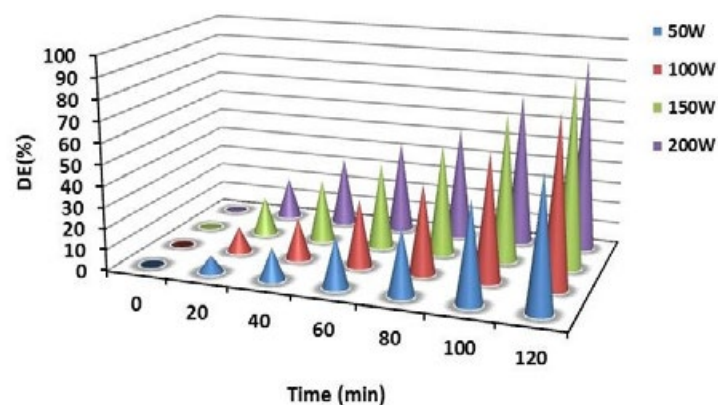


Fig.12. Influence of ultrasound power on the degradation ratio of RRed 43 by 8% Eu-doped CdSe. [RRed 43]₀ = 10 mg/L, [Catalyst]₀ = 1.5 g/L,

the sonication power from 50 to 200 W/L, as seen in Fig. 12. By increasing the ultrasonic power, the generation of the $\bullet\text{OH}$ radicals elevates, resulted in enhanced degradation ratio. Besides,

great power led to the enhancement of solution disturbance, and consequently, promotion the rate of mass transfer for dye, intermediates and reactive species between the bulk solution and

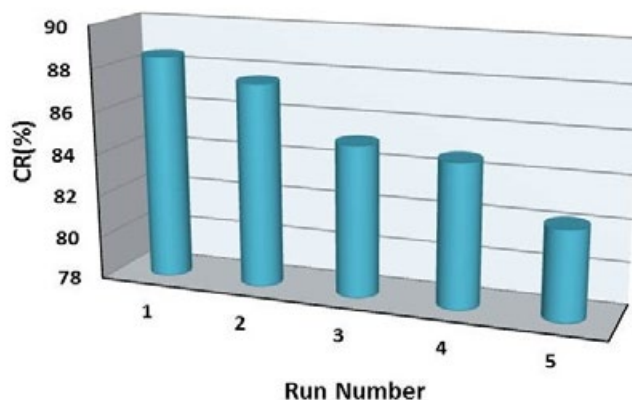


Fig. 13. Reusability of Eu-doped CdSe within five consecutive runs.

surface of the nanocatalyst [25]. Considering the small difference of degradation ratio between 150 and 200 W, we set the experiments on 150 W for energy saving.

Photocatalyst recycling and photostability

Fig. 13 shows the reusability of 8% Eu-doped CdSe was tested in the presence of 1.5 g/L catalyst powder, 10 mg/L dye concentration and the reaction time of 120 min. Following each decolorization test, for the new experiment, the catalyst was gathered and washed with distilled water and dried at 50 °C for 3 h. As is seen in Fig. 13, 8% Eu-doped CdSe sample showed outstanding chemical stability without any notable decaying during catalytic process.

CONCLUSION

In summary, Eu-doped CdSe nanoparticles were synthesized by a simple and environmentally friendly sonochemical method as a novel catalyst. As-synthesized photocatalyst was applied for the sono-photocatalytic decolorization of RRed 43 in aqueous solution. The decolorization efficiency of the synthesized nanoparticles was much higher in sono-photocatalytic process than that of other methods. Elevated degradation ratio was seen in the case of 8% of Eu^{3+} . Various radical scavengers reduce the sonophotocatalytic degradation ratio of RRed 43 especially in the case of 1,4 benzoquinone. The main oxidative species in this process were detected to be h^+_{VB} and superoxide radicals. The results confirmed that Eu-doped CdSe nanoparticles can be used in several experimental cycles without considerable drop in catalytic activity.

ACKNOWLEDGMENT

This work is funded by the grant NRF-2018R1A2B3001246 of the National Research Foundation of Korea.

SUPPLEMENTARY INFORMATION

Supplementary data to this article can be found online at <http://www.nanochemres.org>

CONFLICT OF INTEREST

The authors declare that there is no conflict of interests regarding the publication of this manuscript.

REFERENCES

- Hanifehpour Y, Soltani B, Amani-Ghadim AR, Hedayati B, Khomami B, Joo SW. Synthesis and characterization of samarium-doped ZnS nanoparticles: A novel visible light responsive photocatalyst. *Materials Research Bulletin*. 2016;76:411-21.
- Ahmed S, Rasul MG, Martens WN, Brown R, Hashib MA. Heterogeneous photocatalytic degradation of phenols in wastewater: A review on current status and developments. *Desalination*. 2010;261(1-2):3-18.
- Yuan B, Wang Y, Bian H, Shen T, Wu Y, Chen Z. Nitrogen doped TiO₂ nanotube arrays with high photoelectrochemical activity for photocatalytic applications. *Applied Surface Science*. 2013;280:523-9.
- Daghrir R, Drogui P, Deegan N, El Khakani MA. Electrochemical degradation of chlortetracycline using N-doped Ti/TiO₂ photoanode under sunlight irradiations. *Water Research*. 2013;47(17):6801-10.
- Khataee A, Karimi A, Arefi-Oskoui S, Darvishi Cheshmeh Soltani R, Hanifehpour Y, Soltani B, et al. Sonochemical synthesis of Pr-doped ZnO nanoparticles for sonocatalytic degradation of Acid Red 17. *Ultrasonics Sonochemistry*. 2015;22:371-81.
- Eskandarloo H, Badiei A, Behnajady MA, Ziarani GM. Ultrasonic-assisted sol-gel synthesis of samarium, cerium co-doped TiO₂ nanoparticles with enhanced sonocatalytic

- efficiency. *Ultrasonics Sonochemistry*. 2015;26:281-92.
- Khataee AR, Karimi A, Soltani RDC, Safarpour M, Hanifehpour Y, Joo SW. Europium-doped ZnO as a visible light responsive nanocatalyst: Sonochemical synthesis, characterization and response surface modeling of photocatalytic process. *Applied Catalysis A: General*. 2014;488:160-70.
 - Saharan P, Chaudhary GR, Lata S, Mehta SK, Mor S. Ultra fast and effective treatment of dyes from water with the synergistic effect of Ni doped ZnO nanoparticles and ultrasonication. *Ultrasonics Sonochemistry*. 2015;22:317-25.
 - Villaroel E, Silva-Agreto J, Petrier C, Taborda G, Torres-Palma RA. Ultrasonic degradation of acetaminophen in water: Effect of sonochemical parameters and water matrix. *Ultrasonics Sonochemistry*. 2014;21(5):1763-9.
 - Bansal P, Chaudhary GR, Mehta SK. Comparative study of catalytic activity of ZrO₂ nanoparticles for sonocatalytic and photocatalytic degradation of cationic and anionic dyes. *Chemical Engineering Journal*. 2015;280:475-85.
 - Chakma S, Moholkar VS. Investigation in mechanistic issues of sonocatalysis and sonophotocatalysis using pure and doped photocatalysts. *Ultrasonics Sonochemistry*. 2015;22:287-99.
 - Anju SG, Yesodharan S, Yesodharan EP. Zinc oxide mediated sonophotocatalytic degradation of phenol in water. *Chemical Engineering Journal*. 2012;189-190:84-93.
 - Khataee A, Saadi S, Safarpour M, Joo SW. Sonocatalytic performance of Er-doped ZnO for degradation of a textile dye. *Ultrasonics Sonochemistry*. 2015;27:379-88.
 - Khataee A, Soltani RDC, Karimi A, Joo SW. Sonocatalytic degradation of a textile dye over Gd-doped ZnO nanoparticles synthesized through sonochemical process. *Ultrasonics Sonochemistry*. 2015;23:219-30.
 - Chen M-L, Meng Z-D, Zhu L, Park C-Y, Choi J-G, Ghosh T, et al. Synthesis of Carbon Nanomaterials-CdSe Composites and Their Photocatalytic Activity for Degradation of Methylene Blue. *Journal of Nanomaterials*. 2012;2012:1-7.
 - Biswal N, Parida KM. Enhanced hydrogen production over CdSe QD/ZTP composite under visible light irradiation without using co-catalyst. *International Journal of Hydrogen Energy*. 2013;38(3):1267-77.
 - Raevskaya AE, Stroyuk AL, Kuchmiy SY, Azhniuk YM, Dzhagan VM, Yukhymchuk VO, et al. Growth and spectroscopic characterization of CdSe nanoparticles synthesized from CdCl₂ and Na₂SeSO₃ in aqueous gelatine solutions. *Colloids and Surfaces A: Physicochemical and Engineering Aspects*. 2006;290(1-3):304-9.
 - Robel I, Subramanian V, Kuno M, Kamat PV. Quantum Dot Solar Cells. Harvesting Light Energy with CdSe Nanocrystals Molecularly Linked to Mesoscopic TiO₂ Films. *Journal of the American Chemical Society*. 2006;128(7):2385-93.
 - Zhou M, Han D, Liu X, Ma C, Wang H, Tang Y, et al. Enhanced visible light photocatalytic activity of alkaline earth metal ions-doped CdSe/rGO photocatalysts synthesized by hydrothermal method. *Applied Catalysis B: Environmental*. 2015;172-173:174-84.
 - Hamnabard N, Hanifehpour Y, Khomami B, Woo Joo S. Synthesis, characterization and photocatalytic performance of Yb-doped CdTe nanoparticles. *Materials Letters*. 2015;145:253-7.
 - Khataee A, Khataee A, Fathinia M, Hanifehpour Y, Joo SW. Kinetics and Mechanism of Enhanced Photocatalytic Activity under Visible Light Using Synthesized PrxCd1-xSe Nanoparticles. *Industrial & Engineering Chemistry Research*. 2013;52(37):13357-69.
 - Liang C-H, Li F-B, Liu C-S, Lü J-L, Wang X-G. The enhancement of adsorption and photocatalytic activity of rare earth ions doped TiO₂ for the degradation of Orange I. *Dyes and Pigments*. 2008;76(2):477-84.
 - Wang T, Jin Z, Liu T, Li W, Ni Y. Nanosized CdSe Particles Synthesized by an Air Pressure Solution Process Using Ethylene-Glycol-Based Solvent. *Journal of the American Ceramic Society*. 2010:no-no.
 - Subila KB, Kishore Kumar G, Shivaprasad SM, George Thomas K. Luminescence Properties of CdSe Quantum Dots: Role of Crystal Structure and Surface Composition. *The Journal of Physical Chemistry Letters*. 2013;4(16):2774-9.
 - Khataee A, Saadi S, Vahid B, Joo SW, Min B-K. Sonocatalytic degradation of Acid Blue 92 using sonochemically prepared samarium doped zinc oxide nanostructures. *Ultrasonics Sonochemistry*. 2016;29:27-38.